Science of the Total Environment 651 (2019) 1639–1651

Contents lists available at ScienceDirect

Science of the Total Environment

journal homepage: www.elsevier.com/locate/scitotenv

Relation of El Niño and La Niña phenomena to precipitation, evapotranspiration and temperature in the Amazon basin

Marks Melo Moura, Alexandre Rosa dos Santos *, José Eduardo Macedo Pezzopane, Rodrigo Sobreira Alexandre, Samuel Ferreira da Silva, Stefania Marques Pimentel, Maria Sueliane Santos de Andrade, Felipe Gimenes Rodrigues Silva, Elvis Ricardo Figueira Branco, Taís Rizzo Moreira, Rosane Gomes da Silva, José Romário de Carvalho

Federal University of Espírito Santo/UFES, Center of Agricultural Sciences and Engineering, Alto Universitário, s/n 29500-000 Alegre, ES, Brazil

HIGHLIGHTS

- Changes in precipitation, evapotranspiration and temperature of the Amazon basin were observed.
- Climatic variables were compared in the periods of El Niño, La Niña and Neutral phenomena.
- The variables precipitation, temperature and evapotranspiration were reduced or increased as a result of La Niña or El Niño.
- The methodology can be adapted to other variables and areas different.

GRAPHICAL ABSTRACT

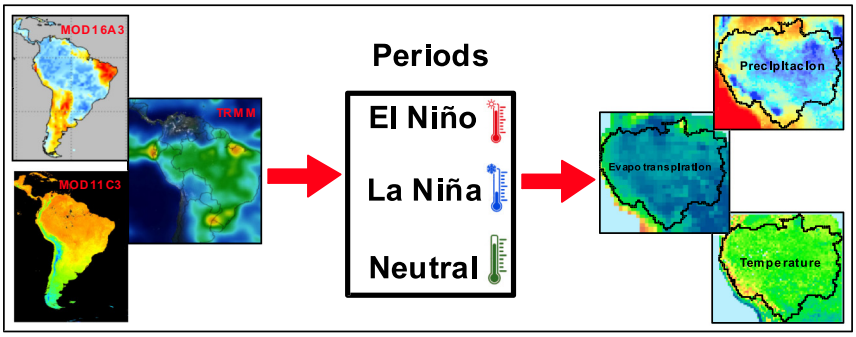

ARTICLE INFO

Article history:
Received 13 June 2018
Received in revised form 28 August 2018
Accepted 18 September 2018
Available online 19 September 2018

Editor: José Virgílio Cruz

Keywords:
Remote sensing
Climate change
Temporal analysis
La Niña
El Niño

ABSTRACT

Weather phenomena El Niño and La Niña are observed by meteorological variables, which allows you to track climate change and its possible effects in certain regions. The objective of this study was to analyze the behavior of rainfall, temperature and evapotranspiration in the Amazon river basin (Latitudes 5° N to 20° S and Longitudes 50° W to 80° W), comparing them with the occurrence of El Niño and La Niña phenomena, from January 2000 to December 2016. The values referring to the meteorological variables were obtained from the TRMM and MODIS orbital sensors. After data pre-processing, the data were separated into monthly and annual scales and per period according to the presence or absence of El Niño and La Niña phenomena. Based on the results obtained, it was observed that the studied variables were affected by modification of both phenomena. The modifications are more noticeable in the distinction between the more and less rainy periods. Among the variables studied, the evapotranspiration was severely affected in the rainiest months, the La Niña phenomenon, and the least rainy months, El Niño. Thus, it was possible to conclude that, in general, the presence of La Niña increased precipitation values in comparison to the Neutral period, but the inverse occurs in the presence of El Niño. The methodology applied in the present study was adequate for the analysis of the modifications of the meteorological variables coming from the El Niño and La Niña phenomena, being able to be adapted to other variables and regions.

© 2018 Elsevier B.V. All rights reserved.

* Corresponding author.
E-mail address: alexandre.santos@pq.cnpq.br (A.R. dos Santos).

https://doi.org/10.1016/j.scitotenv.2018.09.242
0048-9697/© 2018 Elsevier B.V. All rights reserved.

1. Introduction

The uses of remote sensing techniques applied to environmental studies have spread and improved, being able to analyze and characterize the variables environmental processes. Several climatic variables can be obtained or estimated by means of orbital data, some of them with long time series, which facilitates the observation of characteristics over time.

In addition, the time series can be repeatedly monitored in large areas, by the same sensor, with constant time intervals, an attribute that Moreira (2011) cites as the main characteristic of orbital data. Another point addressed by the author is the relative ease in obtaining and manipulating the data, and the varied results that can be achieved.

Therefore, time series are fundamental to observe phenomena that do not have definite seasonality, such as the El Niño (EN) and La Niña (LN) phenomena, which occur at indefinite intervals. Such events are the main sources of particular interannual changes in the climate all regions of the planet (Almeida et al., 2017; Trenberth, 1997). These phenomena alter pluviometric regimes, causing several problems in Brazilian regions, such as extreme drought events in northern Brazil, specifically in the Amazon (Marengo et al., 2008), changes in the pluviometric regime in the southeastern region (Fernando et al., 2013) and the western center (Oliveira et al., 2015).

The greatest impacts observed in the Amazon region, caused by the phenomena EN/LN, are changes in pluviometric and fluviometric regimes. Flood and drought events cause changes in the frequency and intensity of rainfall and, consequently, affect river levels. These alterations lead to changes in riparian communities, vegetation, economic activities and especially in the region's climate (Li et al., 2010).

The Amazon rainforest, through vegetation, has a strong influence on evapotranspiration processes and, consequently, on the hydrological cycle, besides contributing to the interception of rainfall and reduction of the surface runoff process. However, this dynamics is affected by several meteorological variables (Alves and Pérez-Cabello, 2017). In this way, low rainfall indices for prolonged periods together with high temperatures, tend to reduce vegetative vigor (Ponzoni et al., 2012), increasing evapotranspiration (dos Santos et al., 2017). In this context, monitoring climatic variables over time is essential to prevent or predict extreme events. By observing these variables together with the EN/LN phenomena, it is possible to comprehend the variability of these events.

Among the variables that compose the hydrological cycle of the region, one of the most important is evapotranspiration, because of the variables that determines the replenishing of aquifers, the carbon cycle and surface flow (Lin et al., 2017). In this context, Ayala et al. (2016) emphasize that evapotranspiration has been gradually modified due to anthropogenic pressures on vegetation, air, soil and ocean temperatures. Given its importance to the world, the Amazon river basin, which extends through 9 Brazilian states and 8 other South American countries, needs to be studied, especially in terms of its meteorological variables and their possible modifications over of the years. These studies are essential both to monitor and prevent possible natural disasters (Serrão et al., 2015). Thus, the objective of this research was to analyze the behavior of rainfall, temperature and evapotranspiration in the Amazon river basin, relating this behavior to the occurrence of El Niño and La Niña climatic phenomena between January 2000 and December 2016.

2. Material and methods

2.1. Location of study area

The Amazon river basin, the largest in the world in extension with an approximate area of 6.2×10^6 km^2, is located between Latitudes 5° N to 20° S and Longitude 50° W to 80° W (Fig. 1). Its geographical distribution covers seven countries: Brazil (63%), Peru (17%), Bolivia (10%), Venezuela (7%), Colombia (5.8%), Ecuador (2.2%) and Guyana (0.3%) (Viers et al., 2005). Due to its size and location, this basin presents great climatic diversity, however its climate is primarily determined by its tropical location. Given this, its average rainfall is approximately 2200 mm year^{-1}, which originates from the South Atlantic and the evapotranspiration of the Amazon rainforest.

2.2. Data acquisition and processing

The elaboration of the present research and the data used together with its subsequent processing are shown in the methodological flowchart (Fig. 1) and detailed in sequence.

2.2.1. Pluviometric precipitation data

Rainfall data was obtained through the Tropical Rainfall Measuring Mission (TRMM) sensor. For the period studied, it was necessary to acquire 204 monthly precipitation images (January 2000 to December 2016) available free of charge at the site https://disc.gsfc.nasa.gov/TRMM. The TRMM data, product 3B43, is available on a global scale, with a spatial resolution of 0.25° (approximately 27.83 km) and for the purpose of comparison with the other variables (evapotranspiration and temperature) the monthly temporal resolution was chosen. Correct acquisition of precipitation data requires preprocessing the images. Therefore, the units were initially converted from millimeters per hour (mm hr −1) into millimeters (mm) using the map algebra function by multiplying the total hours of the month by the pixel value, taking into account leap years.

2.2.2. Earth surface temperature

The product MOD11C3 of the MODIS sensor was used to obtain land surface temperature (LST), with monthly temporal resolution and spatial resolution of 0.05° (approximately 5.56 km). The MODIStsp 1.3.0® software was used to download, reproject, convert the format and join the images forming a mosaic of the area of interest (the Amazon river basin). Each year studied contained 12 LST images, except for 2000 that only had 11 values, since the images only began to be captured by the MODIS sensor in February of that year, therefore excluding January.

During initial image processing, a reclassification of the Quality Assurance (QA) images was performed. For this study, pixels with values 0 and 1 (good quality and intermediate quality respectively) were used, thus excluding pixels 2 and 3. After the reclassification values 0 and 1 were replaced by 0, and Nodata values (without data) were entered for the pixels with values 2 and 3 as shown in Table 1. The QA product was used to correct the images, removing all the coverings of the earth that are not snow, that is to say, have been removed possible layers of water that the sensor initially interpreted as snow cover.

After reclassification, the LST and QA images were overlapped, thus generating an LST image with reliable temperature values. The LST raw data was originally in Kelvin (K), its being necessary to convert it into degrees Celsius (°C) (Eq. 1).

$$T\left[^{\circ}C\right] = (T[K] \cdot 0.02) - 273.15 \quad (1)$$

where:T[°C] = temperature in degrees CelsiusT[K] = temperature in Kelvin0.02 scale factor used for the LST product of the MODIS sensor.

2.2.3. Evapotranspiration

The data on total evapotranspiration was obtained through the product MOD16A2, where the spatial resolution of 500 m was used, with monthly temporal resolution. The data was obtained free of charge at http://files.ntsg.umt.edu. For the study period, 204 images were necessary (from 2000 to 2016). Modifications were firstly made to the image pixels according to their initial values. In this way, the pixels with values expressed in Table 2 were replaced by pixels without data (NoData).

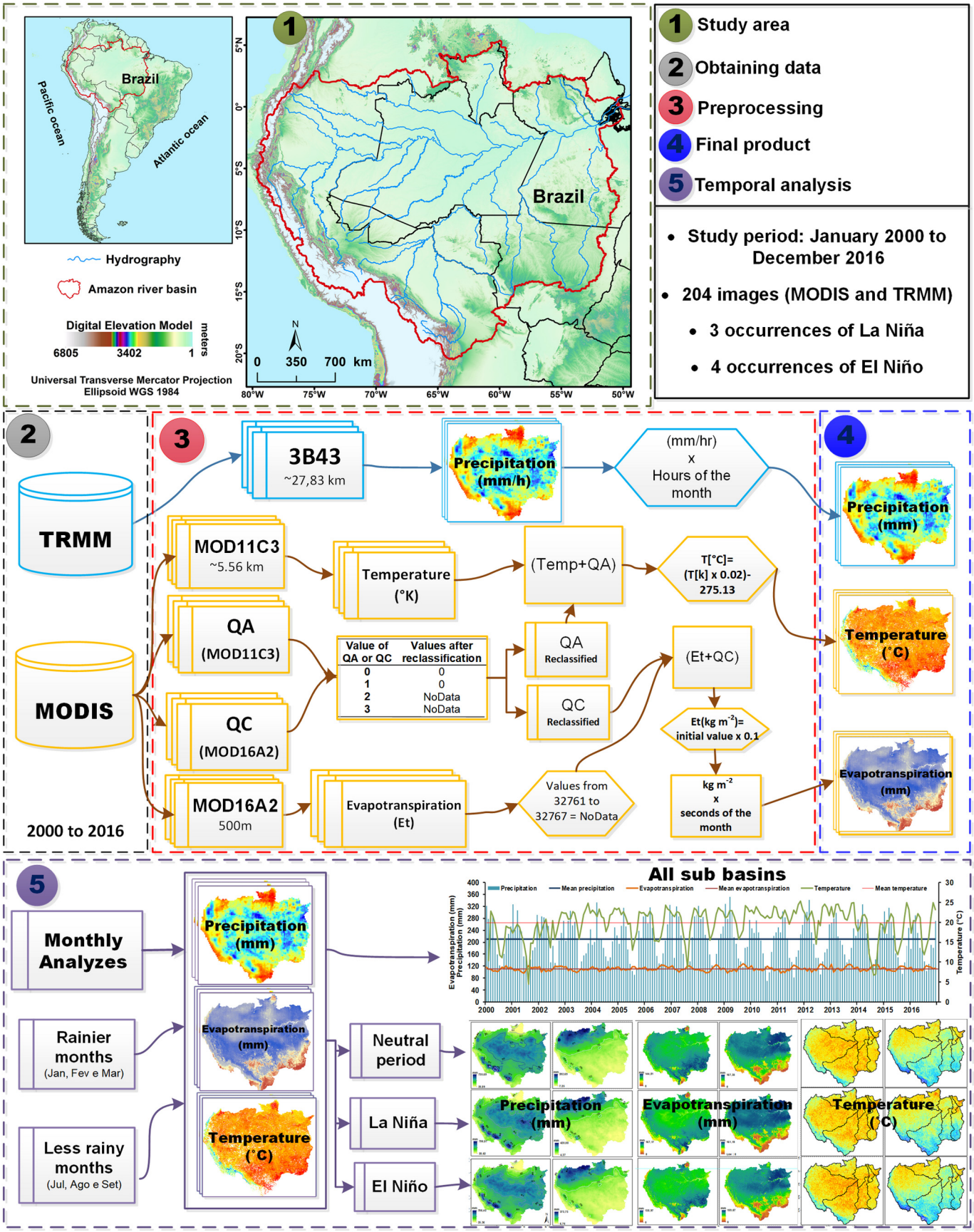

Fig. 1. Flowchart representing the study area and summary of the methodological steps used to process the orbital data (TRMM and MODIS), and temporal analyses performed. QC: Quality Control; QA: Quality Assurence.

Table 1
Specification of the quality of the pixels for the product MOD11C3, the first values are in binary basis, while their respective values are in decimal base in the brackets.
Source: adapted from Wan (2013).

Data sets	Description	Value after reclassification
QA (mandatory quality assurence)	00 - (0) - Pixel produced, good quality, not necessary to examine more detailed QA	0
	01 - (1) - Pixel produced, unreliable or unquantifiable quality, recommend examination of more detailed QA	0
	10 - (2) - Pixel not produced due to cloud effects	NoData
	11 - (3) - Pixel not produced primarily due to reasons other than cloud (such as ocean pixel, poor input data)	NoData

After assigning the NoData values, the pixels were corrected using the Quality Control (QC) data, so this by-product is necessary to correct the images by removing all pixels with inaccurate data. Table 3 shows the initial pixel values and after reclassification to the QC by-product of MOD16A2. Subsequently reclassified QC was used for the correction of evapotranspiration images. The final data is in the unit kg m^{-2} s^{-1} (equivalent to mm s^{-1}). For conversion into millimeters (mm) it is necessary to multiply by the total seconds in a month, taking leap years into consideration.

2.2.4. El Niño and La Niña events

In order to monitor the EN/LN events, oceanic information is adopted, since it is considered a great precursor and essential to understand these phenomena (Fujii et al., 2012). By means of these indicators, it was possible to evaluate the seasonality and characteristics intrinsic to the phenomenon, which usually begin in the second half of a given year and finish at the end of the first half of the following year. Many indicators have been developed to monitor EN/LN phenomena, with an emphasis on the Southern Oscillation Index (SOI), which is based on the average ocean temperature. When the index is positive, the temperature of the Pacific Ocean is higher than normal, and for the negative index, the opposite occurs.

By obtaining the three-month moving average of the temperature, it is possible to know if EN/LN events are occurring or not. If the average exceeds +0.5 °C for at least five consecutive months there is an EN event and if it is less than −0.5 °C there is a La Niña event. The absence of either condition is called a neutral year, as shown in Table 4 (Trenberth, 1984). The SOI values were classified according to degrees of intensity, and can be characterized as weak to very strong, as shown in Table 5 (Trenberth, 1997; Trenberth and Stepaniak, 2001). In Table 6, it is possible to observe the series of years where anomalies were registered in the ocean surface temperatures, indicating the occurrence of El Niño and La Niña events during the period between 2000 and 2016 and their respective intensities.

2.2.5. Monthly data analysis

The meteorological variables (precipitation, temperature and evapotranspiration) were processed to obtain the mean monthly values of the pixels for the EN/LN phenomena. To compare the monthly variations of meteorological data, a historical average was performed for each variable, considering the period studied (2000 to 2016). In this way, we can analyze the positive and negative effects of the phenomena (El Niño and La Niña) on the variables, assuming as a basic parameter the historical average obtained.

Table 2
Pixel values and their respective coverage.
Source: adapted from Running et al. (2017).

Value	Land cover assigned	Value after reclassification
32,767	Fill value	NoData
32,766	Perennial salt or Water bodies	NoData
32,765	Barren,sparse veg (rock, tundra, desert)	NoData
32,764	Perennial snow, ice	NoData
32,763	Permanent wetlands/inundated marshland	NoData
32,762	Urban/built-up	NoData
32,761	Unclassified or not able to determine	NoData

Table 3
Pixel quality specification for product MOD16A2.
Source: adapted from Running et al. (2017).

Data sets	Description	Value after reclassification
Quality control (QC)	'00' = 0 - Significant clouds not present (clear)	0
	'01' = 1 - Significant clouds were present	0
	'10' = 2 - Mixed cloud present on pixel	NoData
	'11' = 3 - Cloud state not defined, assumed clear	NoData

2.2.6. Analysis of variations during high and low precipitation periods

In order to compare changes in the meteorological variables (precipitation, temperature and evapotranspiration) due to EN/LN phenomena, the months with the highest rainfall intensities (January, February and March) and lower intensities (July, August and September) were selected, according to Foley et al. (2002). In addition, the periods were defined according to the occurrence or not of the studied phenomena, so that the means were compared between the years with influence of EN, LN and Neutral periods, resulting in six maps for the LN, EN and Neutral period variables, during times of higher and lower precipitation intensity. To verify the increase or reduction of variables, a subtraction between their averages was performed in periods with and without occurrence of the studied phenomena, resulting in four different maps.

3. Results

3.1. Monthly and annual analyses of meteorological variables

The mean values of rainfall, evapotranspiration and temperature were 185.03 mm, 110.11 mm and 20.82 °C, respectively (Fig. 2), with the respective standard deviations 78.01 mm, 6.22 mm and 4.49 °C. It is possible to observe, in the Fig. 2, the monthly precipitation data, in which the lowest observed values were 43.28 mm (2015), 65 mm (2001), 66.85 mm (2000), 68.53 mm (2015), 71.19 mm (missing the year), 72.59 mm (2007), 73.29 mm (2009), 73.62 mm (2012), 73.91 mm (2015) and 74.62 mm (2002), six of which were associated with the presence of the EN phenomenon, with the presence of the LN phenomenon and none in neutral periods.

The lowest monthly temperature values observed (Fig. 2) in the period studied were: 5.22 °C (2014), 5.89 °C (2001), 6.86 °C (2014), 7.95 °C (2015), 9.59 °C (2015), 9.66 °C (2014), 10 °C (2015), 10.9 °C (2001), 11.36 °C (2007) and 12.1 °C (2001) and the highest 29.18 °C, 28.73 °C, 28.44 °C, 28.39 °C, 28.29 °C, 27.7 °C, 27.48 °C, 27.23 °C, 27.22 °C and 27.01 °C, all during 2016, the year that presented a EN phenomena of greatest intensity.

It is worth noting that among the ten largest months of precipitation, six were observed in the presence of EN, three in LN and only one during Neutral periods, being: 331.58 mm (2009), 327.54 mm (2011), 326.88 mm (2005), 318.99 mm (2014), 318.98 mm (2005), 317.88 mm (2004), 316.91 mm (2001), 316.14 mm (2000), 315.92 mm (2008) and 314.88 mm (2016), respectively. For the data of the monthly evapotranspiration variable (Fig. 2), the lowest observed values varied between 95.76 mm (2001) and 100.62 (2012), with eight and two occurrences in the LA and EN phenomena, in that order. In relation to the highest values obtained, it was observed that six occurred in years with EN, two in LN and two in Neutral periods, varying from 121.23 mm (2009) and 127.65 mm (2009).

Table 4
SOI values for the years 2000 to 2016, where the values in blue indicate negative means in the three months characterizing La Niña events and values in red indicate El Niño events. The other years present values that characterize neutrality, not indicating either of the two events.
Source: adapted from NOAA (2017).

Year	DJF[1]	JFM[2]	FMA[3]	MAM[4]	AMJ[5]	MJJ[6]	JJA[7]	JAS[8]	ASO[9]	SON[10]	OND[11]	NDJ[12]
2000	**−1,6**	**−1,4**	**−1,1**	**−0,9**	**−0,7**	**−0,7**	**−0,6**	**−0,5**	**−0,6**	**−0,7**	**−0,8**	**−0,8**
2001	**−0,7**	**−0,6**	**−0,5**	−0,3	−0,2	−0,1	0	−0,1	−0,1	−0,2	−0,3	−0,3
2002	−0,2	−0,1	0,1	0,2	0,4	**0,7**	**0,8**	**0,9**	**1**	**1,2**	**1,3**	**1,1**
2003	**0,9**	**0,6**	0,4	0	−0,2	−0,1	0,1	0,2	0,3	0,4	0,4	0,4
2004	0,3	0,2	0,1	0,1	0,2	0,3	**0,5**	**0,7**	**0,7**	**0,7**	**0,7**	**0,7**
2005	**0,6**	**0,6**	**0,5**	**0,5**	0,4	0,2	0,1	0	0	−0,1	−0,4	−0,7
2006	−0,7	−0,6	−0,4	−0,2	0	0,1	0,2	0,3	**0,5**	**0,8**	**0,9**	**1**
2007	**0,7**	0,3	0	−0,1	−0,2	−0,2	−0,3	**−0,6**	**−0,8**	**−1,1**	**−1,2**	**−1,3**
2008	**−1,4**	**−1,3**	**−1,1**	**−0,9**	**−0,7**	**−0,5**	−0,3	−0,2	−0,2	−0,3	−0,5	−0,7
2009	−0,8	−0,7	−0,4	−0,1	0,2	0,4	**0,5**	**0,6**	**0,7**	**1**	**1,2**	**1,3**
2010	**1,3**	**1,1**	**0,8**	**0,5**	0	−0,4	**−0,8**	**−1,1**	**−1,3**	**−1,4**	**−1,3**	**−1,4**
2011	**−1,3**	**−1,1**	**−0,8**	**−0,6**	−0,3	−0,2	−0,3	**−0,5**	**−0,7**	**−0,9**	**−0,9**	**−0,8**
2012	**−0,7**	**−0,6**	**−0,5**	−0,4	−0,3	−0,1	0,1	0,3	0,4	0,4	0,2	−0,2
2013	−0,4	−0,5	−0,3	−0,2	−0,2	−0,2	−0,2	−0,2	−0,2	−0,2	−0,2	−0,3
2014	−0,5	−0,6	−0,4	−0,2	0	0	0	0	0,2	0,4	0,6	0,6
2015	0,5	0,4	**0,5**	**0,7**	**0,9**	**1**	**1,2**	**1,5**	**1,8**	**2,1**	**2,2**	**2,3**
2016	**2,2**	**2**	**1,6**	**1,1**	**0,6**	0,1	−0,3	−0,6	−0,8	−0,8	−0,8	−0,7

[1]December of the previous year, January and February; [2]January, February and March; [3]February, March and April; [4]March, April and May; [5]April, May and June; [6]May, June and July; [7]June, July and August; [8]July, August and September; [9]August, September and October; [10]September, October and November; [11]October, November and December; and [12]November, December and January of the following year.

The accumulated totals for annual precipitation and their corresponding average (2220.31 mm) are presented in Fig. 3. Compared with the average, the greatest reductions were by 346.62 mm(2015) and −150.52 mm (2016). Regarding the largest increases, the results were 244.91 and 178.05 mm, for 2000 and 2008, respectively.

As for annual temperature averages compared to the historical average (20.82 °C), there were greater reductions by 4.95 °C and 5.25 °C for 2001 and 2014, respectively. The largest increases were observed in 2013 (3.19 °C) and 2016 (6.81 °C), as shown in Fig. 3A and E. In terms of evapotranspiration (Fig. 3. changes were also observed in relation to the historical average (110.11 mm). These changes were observed with greater intensity in 2000 (−4.34 mm), 2001 (−3.73 mm), 2014 (3.43 mm) and 2009 (3.26 mm). In Fig. 3, E and F, the results of the variables studied between 2000 and 2016 are shown. A negative tendency of −395.43 mm for precipitation is observed, whereas the temperature and the evapotranspiration presented positive trends of 9.78 °C and 6.53 mm, respectively.

3.2. Alteration of precipitation caused by El Niño and La Niña phenomena

In Fig. 4A, the rainfall average for the Neutral periods (without occurrence of phenomena) was observed in the months with the highest precipitation rates (January, February and March), with values varying from 25.89 mm in the northern region of the Amazon basin to 735.69 mm in the southwestern region. In this period the mean obtained was 275.63 mm with a standard deviation of 80.79 mm. For the rainy months in years with the occurrence of the LN phenomenon, a variation average of 28.62 mm to 786.87 mm presented an increase in relation to the minimum and maximum precipitations of the Neutral period. In this way, this allows us to conclude that the occurrence of the phenomenon raised the means to 278.90 mm with a standard deviation of 82.33 mm (Fig. 4B). By contrast, months with precipitation showing the presence of EN phenomenon (Fig. 4C) were affected by reductions in precipitation totals when compared to the Neutral and LN periods, therefore varying from 25.36 to 706.43 mm, resulting in an average of 259.97 mm and standard deviation of 78.05 mm.

Fig. 4F, G and H show the precipitation variation in the months with the lowest precipitation (July, August and September). Above all, Fig. 4F presents the precipitation values during Neutral periods, ranging from 7.25 to 392.69 mm, obtaining an average of 102.91 mm and a standard deviation of 79.16 mm. During this period rainfall was observed in the northwest region of the basin when compared to the rainy season (Fig. 4A). Additionally, a variation in precipitation during the occurrence of the LN phenomenon can be seen in Fig. 4G, with values varying from 4.27 to 420.08 mm. Therefore, the presence of the phenomenon contributed to a decrease of the mean (97.8 mm), with a standard deviation of 78.13 mm.

For the years showing the presence of the EN phenomenon, the values decreased in comparison with the Neutral periods, with precipitation varying from 6.76 to 373.73 mm, resulting in an average of 99.82 mm with a standard deviation of 77.77 mm. These results correspond to a decrease of the average in relation to the Neutral and LN periods. For the years characterized by EN, the values decreased in relation to the Neutral periods, with rainfall varying from 6.76 to 373.73 mm, resulting in an average of 99.82 mm with a standard deviation of 77.77 mm, showing a decrease in the mean in terms of the Neutral and LN periods. The rainier and less rainy periods showing presence of the LN phenomenon are shown in Fig. 4D and I, respectively. It can be observed that during the rainy season there were reductions of up to

Table 5
Classification of the intensity of El Niño and La Niña events according to the Southern Oscillation Index (SOI).
Source: adapted from Trenberth (1997); Trenberth and Stepaniak (2001).

Phenomenon	SOI	Intensity
El Niño	0,5 a 0,9	Weak
	1,0 a 1,4	Moderate
	≥1,5	Strong
La Niña	−0,5 a −0,9	Weak
	−1,0 a −1,4	Moderate
	≤ −1,5	Strong

Table 6
Years of occurrence of the phenomena in the period from 2000 to 2016.
Source: adapted from ggweather (2008) and INPE (2017).

Phenomenon	Years of occurrence	Intensity
La Niña	2000–2001	Weak
El Niño	2002–2003	Moderate
El Niño	2004–2005	Weak
La Niña	2007–2008	Moderate
El Niño	2009–2010	Moderate
La Niña	2010–2011	Moderate
La Niña	2011–2012	Weak
El Niño	2015–2016	Strong

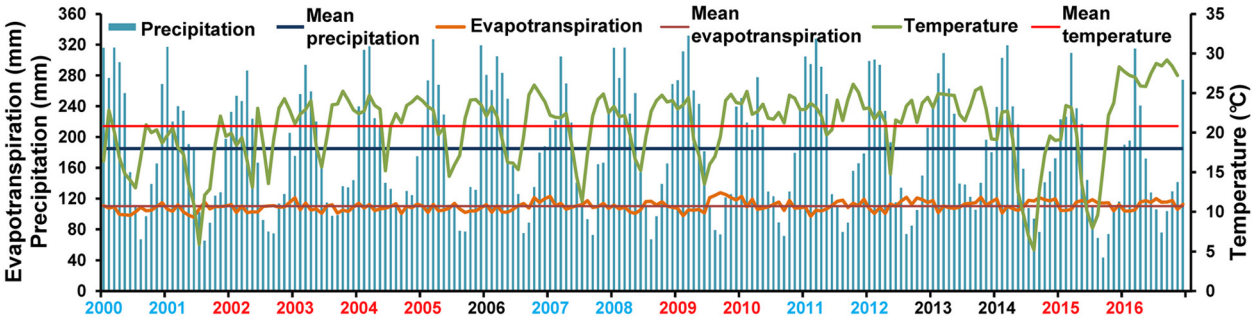

Fig. 2. Monthly and general mean values of precipitation, evapotranspiration and temperature for the Amazon basin (2000 to 2016); blue years represent La Niña presence, red years El Niño presence and black years are Neutral.

71 mm and increases of 120 mm, while in the less rainy months the reductions were as much as 70 mm and increases of 50 mm. The presence of the EN phenomenon indicated that the levels of reduction and increase varied from 25 mm to −68 mm in the rainier months (Fig. 4E) and 35 mm to −36 mm in the less rainy months (Fig. 4J).

3.3. Changes in temperatures caused by El Niño and La Niña phenomena

Fig. 5A, B and C show the spatial variations of temperatures in months with higher rainfall intensities due to EN, LN and Neutral periods. It was found that the average temperature in the rainiest months without presence of the phenomena studied was 21.46 °C with standard deviation of 3.95 °C. The highest temperatures were observed in the Central and Southeastern regions with values varying between 25 and 30 °C (Fig. 5A). In the rainy periods with presence of LN (Fig. 5B) there was a spatial variation of the temperatures compared to the Neutral period, mainly in the northeast and southwest of the Amazon river basin with an average value of 21.41 °C and standard deviation of 4.12 °C. These results show a decrease in relation to the periods without occurrence of the phenomenon (Fig. 5A).

In relation to the changes caused by the EN phenomenon in the rainiest months (Fig. 5C), there is an increase in the amplitudes between 25 and 35 °C, especially in the central region when compared to the other periods. In the less rainy months under the influence of the EN phenomenon (Fig. 5H), the lowest temperatures of the studied period were observed in the south and southwest regions. The highest temperatures in the north and northeast of the basin were observed in the less rainy months with the presence of LN (Fig. 5G). The difference observed between the months with higher and lower precipitation intensities under the influence of the LN phenomenon are presented in Fig. 5D and I, where there was an increase of up to 11 °C in some areas for months with higher precipitation and 14 °C for months of lower precipitation. It was observed that during months with lower rainfall intensity (Fig. 5I), there was a decrease in temperature, dropping by as much as 13 °C, while during months with higher rainfall, the reductions were – as much as 16 °C (Fig. 5D). In Fig. 5E, the differences between the EN phenomenon and the Neutral period in the rainier months are presented. It is possible to observe increases of up to 11 °C and reductions of as much as 7.5 °C for the months influenced by the EN phenomenon. Similar values were also observed in the less rainy periods (Fig. 5J), where decreases were as much as 8.1 °C and increases up to 8.6 °C.

3.4. Alteration of evapotranspiration caused by El Niño and La Niña phenomena

Fig. 6 shows the values of evapotranspirations in the months of the year that are characterized by the presence of EN (less rainy) and LN (rainier) phenomena. Additionally, the spatial variation of evapotranspiration during the period of LN in the rainiest months, with a maximum of 167.17 mm and a mean of 111.45 mm is shown in Fig. 6B. For the Neutral period (Fig. 6A) the maximum value was 144.80 mm with a mean of 103.47 mm. The comparison of these Figures with Fig. 6C, in which the evapotranspiration variation due to the influence of the EN phenomenon is shown, presented a reduction of the values, so that the maximum was reduced to 138.97 mm and the average obtained during this period was 96.01 mm.

Evapotranspiration was reduced in the presence of EN in the less rainy months (Fig. 6), compared to LN (Fig. 6G) and Neutral periods (Fig. 6F). Given the non-occurrence of the Neutral period phenomenon, the maximum and average evapotranspiration obtained were 167.35 mm and 106 mm. In the presence of LN, the maximum value of 161.19 mm was observed for evapotranspiration, with a mean value of 106.85 mm. During EN, the influence on the maximum and average observed was 159.67 mm and 102.6 mm, respectively. The lowest evapotranspiration values were observed in the southern and southeastern regions of the basin during periods with lower rainfall intensities (Fig. 6F, G and H).

In this sense, the differences between the evapotranspiration values under the influence of the EN and LN phenomena are presented in Fig. 6D, I, E and J. It was observed that under La Niña occurrence in rainy periods (Fig. 6D) there was an increase of up to 53 mm of total evapotranspiration in almost the entire basin. Additionally, reductions were observed in the northern part of the basin of as much as 24 mm, different to the southern region where increases between 31 and 53 mm were observed. In this scenario, a variation of 22 mm to −20 mm was observed with the presence of the EN phenomenon in the months with higher rainfall intensities (Fig. 6E). In addition, almost all the basin was characterized by reductions in evapotranspiration from 5 mm to 20 mm. In the months with lower rainfall intensities, the variation was −21 mm to 24 mm (Fig. 6J).

4. Discussion

4.1. Pluviometric precipitation

The monthly precipitation evaluation showed that of the ten events with the lowest rainfall in the period studied, six were associated with the EN and four with LN phenomena, demonstrating that the events influence the monthly averages. Liberato and Brito (2011) and Serrão et al. (2015) identified rainfall events in the Amazon river basin and observed that the precipitation pattern associated with EN refers to drier conditions when compared to neutral years or with the presence of the LN phenomenon, which was observed by the authors with the above-mentioned precipitation deficits ranging from 100 to 200 mm.

Fig. 3. Annual values for precipitation and temperature (A), precipitation and evapotranspiration (B), temperature and evapotranspiration (C), averages and trendlines of precipitation (D), temperature (E) and evapotranspiration (F), years represented with blue, red and black show La Niña, El Niño and neutral periods, respectively.

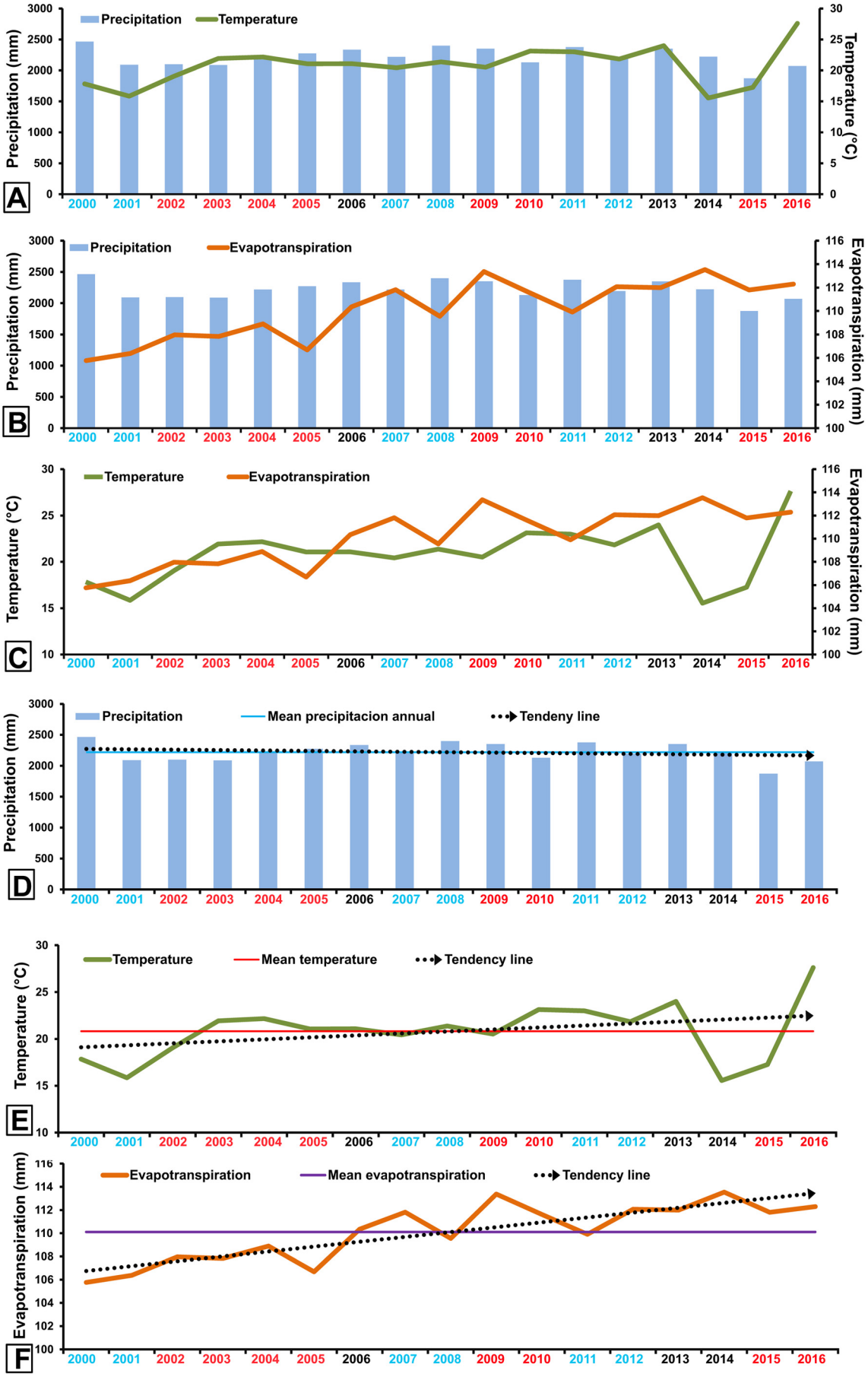
A
Precipitation
Temperature
Precipitation (mm)
Temperature (°C)
B
Precipitation
Evapotranspiration
Precipitation (mm)
Evapotranspiration (mm)
C
Temperature
Evapotranspiration
Temperature (°C)
Evapotranspiration (mm)
D
Precipitation
Mean precipitacion annual
Tendeny line
Precipitation (mm)
E
Temperature
Mean temperature
Tendency line
Temperature (°C)
F
Evapotranspiration
Mean evapotranspiration
Tendency line
Evapotranspiration (mm)
2000 2001 2002 2003 2004 2005 2006 2007 2008 2009 2010 2011 2012 2013 2014 2015 2016

Among the ten highest rainfalls during the period, six were in EN years, three with LN and only one in a Neutral period. Nobre et al. (2013) stated that these above-average precipitation changes may be associated with atmospheric variability caused by phenomena, but at different time scales with local atmospheric effects.

On the one hand, observation of annual rainfall showed values below the historical average in the presence of EN, while in LN the annual totals coincided with the average or exceed it. Therefore, dos Santos et al. (2017) in their studies on extreme drought events in the Amazon, concluded for the same study area that the conditioning factor for water scarcity was the presence of the EN phenomenon. However, some authors argue that events with higher intensities are more noticeable and cause greater rainfall variability in the Amazon region (Huang et al., 2017; Ji et al., 2017).

On the other hand, the temporal analysis of annual cumulative totals showed a decreasing tendency, indicating a reduction of precipitation in the period studied, with a difference of 395.43 mm, or a decrease of approximately 23 mm per year. Estimates of the Intergovernmental Panel on Climate Change (IPCC) showed that for every one Celsius degree of warming total precipitation drops by 5% (IPCC, 2014).

However, the spatial variation of rainfall in the rainier months of the basin without influence of the phenomena, compared to the period with LN presence, showed an increase in rainfall, especially in the southwest, a region where the air masses originating in the Amazon rainforest meet a natural obstacle in the Andes mountain range, causing an accumulation of air masses, being the region presenting the highest rainfall indices. In addition, a reduction of the precipitation values was observed in the presence of the EN phenomenon. However, despite this reduction, there was no interference in its spatial distribution when compared to previous periods. Similar results were observed by de Sousa et al. (2015), where the authors observed that variability was caused by oscillations in the inelastic and annual scales and were connected to each other, modulating the local atmosphere, due to the different phases and intensities of the phenomena.

In the months with the lowest precipitation (July, August and September), under the influence of the LN phenomenon, it was possible to verify an increase in rainfall for maximum values and reduction of minimum values, when compared to the neutral period. Therefore, the precipitation values for the months influenced by the El Niño phenomenon no difference in the spatial distribution of the precipitation. In this way, it can be emphasized that the phenomena did not exert modifications on the spatial distributions of precipitation during the months with higher and lower rainfall levels, however the precipitation totals were modified according to the climatic influence of the phenomena, that is, the LN phenomena increased rainfall while the opposite occurred with EN.

It was observed that both the increases and reductions of the pluviometric precipitation occurred in the presence of both the EN and LN phenomena. It is worth noting that the months with low precipitation rates are characterized by SOI with lower values, conditioned by a reduction in intensity of the phenomenon. Contrary to this, the highest SOI values were obtained in the rainiest months, conditioning more intense periods of the EN phenomenon. Therefore, Nobre et al. (2013) state that the spatial variations caused by the EN and LN phenomena are more evident between the 5°N and 5°S parallels. This occurs because the air mass flows are more intense in this region, corroborating with the variations in the northern part of the basin, where the greatest changes in rainfall indices were observed.

In the months with the highest pluviometric precipitation intensities in the presence of the La Niña phenomenon, a greater increase in precipitation was observed when compared with the EN phenomenon. According to Marengo et al. (2008), these characteristics are related to the changes of the rainy season due to the LN phenomenon, such that the precipitation in a certain place will be affected by a delay of up to 5 months, thereby modifying the rainfall cycle. In general, EN events led to differential alterations in precipitation distribution in the Amazon river basin, in the rainier months. Given this, precipitation was reduced by up to 68 mm, while during less rainy periods the reductions were - as much as 36 mm. Even with the presence of this phenomenon, rainfall increases of 25 to 35 mm were observed for the rainier and less rainy months, respectively.

These results may be related to the different areas of activity of positive sea surface temperature (SST) anomalies in the Central and East Equatorial Pacific. These positive anomalies provoke alterations in the zonal atmospheric circulation (Walker cell), with displacement of the ascending branch to the region of Peru. As a consequence of this phenomenon, the subsiding branch (air flow from top to bottom) of this cell acts more in the eastern sector of the Amazon, thereby reducing the convective activity on the region (de Sousa et al., 2015).

4.2. Temperature

Monthly temperature variability showed that among the 10 events with the lowest temperatures in the studied period, three occurred in years with El Niño, four in LN years and three in Neutral periods. It is worth mentioning that in the ten highest temperatures in the historical series all were associated with the presence of EN, emphasizing the influence of this phenomenon in increasing the values of this variable. It should be noted that this particular event was characterized with strong intensity, which may have accentuated rainfall reductions and, consequently, the increase of monthly temperature averages in this year (Panisset et al., 2017). The observation of the variation of temperature averages in annual scale showed values above the historical average in all years with EN, except during 2015. For the years with LN, the values were very close to the mean, indicating that events with above-average temperatures are associated with the EN phenomenon.

By means of the temporal analysis of the annual averages, a tendency line with an increasing pattern was observed, indicating a temperature increase over the years, with a difference of 9.78 °C between 2000 and 2016, an increase of approximately 0.57 °C every year. These results corroborate the estimates of the Intergovernmental Panel on Climate Change (IPCC), where scenario simulations estimated an increase of 0.5 to 1 °C in South American temperatures between 2015 and 2039 (IPCC, 2014). In relation to the spatial variation of temperature in the rainier months of the basin without the influence of the phenomena compared to the period with LN presence, significant temperature increases or reductions during these periods were not observed. Therefore, this phenomenon does not directly or immediately influence temperature, suggesting that the possible variations occurring in these variables are from other sources of variation (Hua et al., 2017). In the presence of the EN phenomenon, it was possible to observe an increase in temperature, especially in the central part, this variation is a consequence of the weakening of the trade winds (moist), causing hot air masses coming from the Pacific Ocean, creating a pluviometric reduction in the basin and consequently, a temperature rise (Fan et al., 2017; Marengo et al., 2011).

In the months with the lowest rainfall (July, August and September) influenced by the LN phenomenon, it is possible to verify a temperature increase in the north and northeast with values between 25 and 30 °C, an increase of up to 10 °C compared to the Neutral period. The values referring to the months showing an influence of the EN phenomenon are presented, with little difference between this period and the Neutral period, corroborating with the values observed in the monthly analysis where EN did not influence minimum temperature values.

In relation to the differences between the periods in more or less pluviometric precipitation months, it was observed that the increase and reduction occurred in both phenomena (EN and LN). However, during LN periods, reductions varied by as much as 16 °C in months with higher pluviometric precipitation intensities and 13 °C in months with lower pluviometric precipitation. Therefore, LN generated greater temperature reductions in the rainier months, while the highest increases were in the less rainy months (Cai et al., 2014).

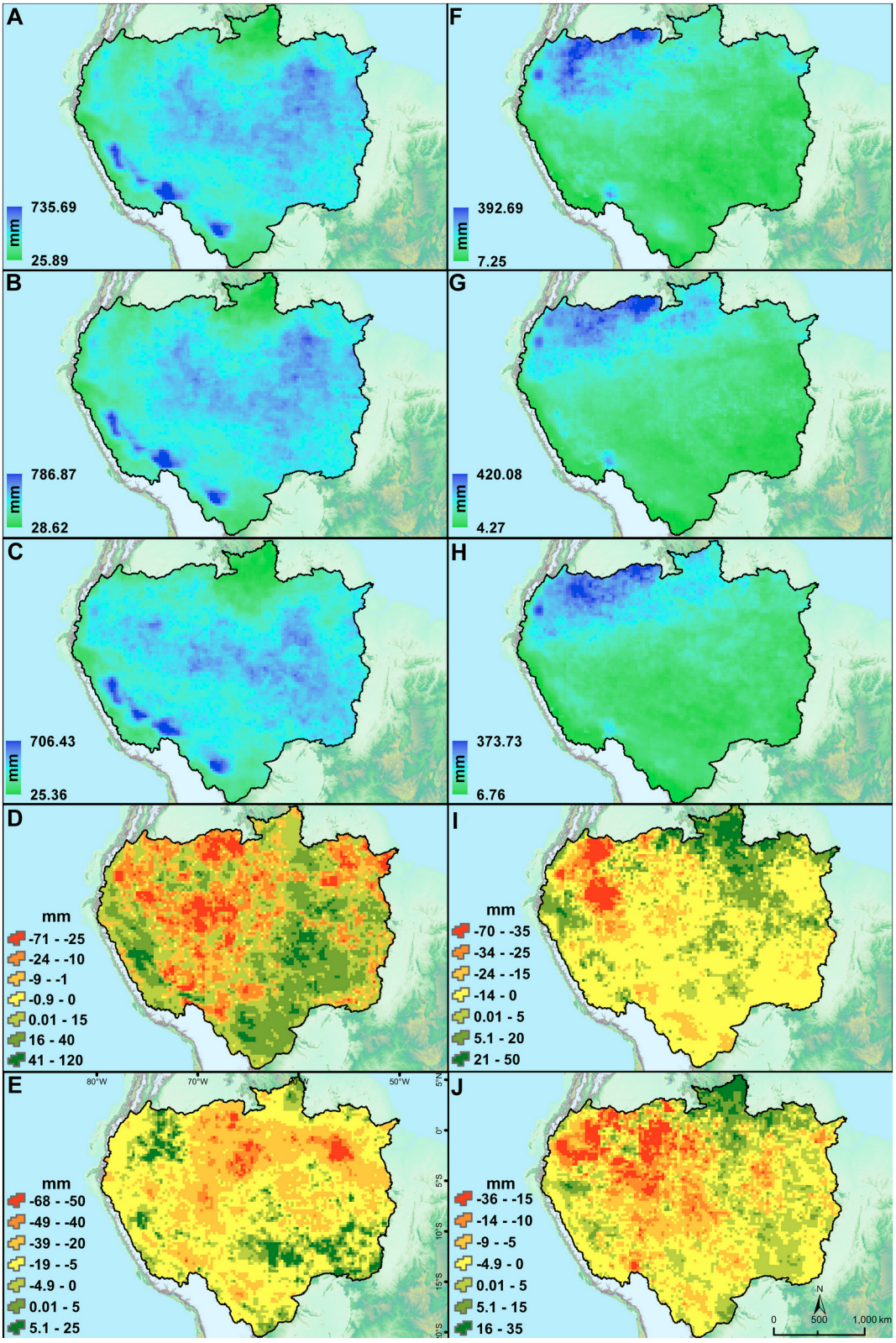

Fig. 4. Variations in precipitation without presence of the phenomena in the rainiest (A) and less rainy (F) months, precipitation with presence of La Niña in rainier (B) and less rainy months (G), precipitation with presence of El Niño in rainier (C) and less rainy (H) months, increase and reduction of precipitation with La Niña presence in the rainiest (g) and least rainy periods (I), El Niño presence in the rainiest (E) and least rainy periods (J).

For the period marked by EN, reductions of up to 7.5 °C were observed for the rainy months and 8.1 °C for the less rainy months, mainly in the southern and southwestern part of the basin and in areas near the Andes mountains. However, the values that characterized temperature increases were similar between EN and LN phenomena. Similar values were observed by Mokhov and Smirnov (2016) in their studies involving variations caused by EN and LN from 1870 to 2014 in the same region. In general, changes in temperature due to phenomena are spatially distributed, with no changes in specific regions.

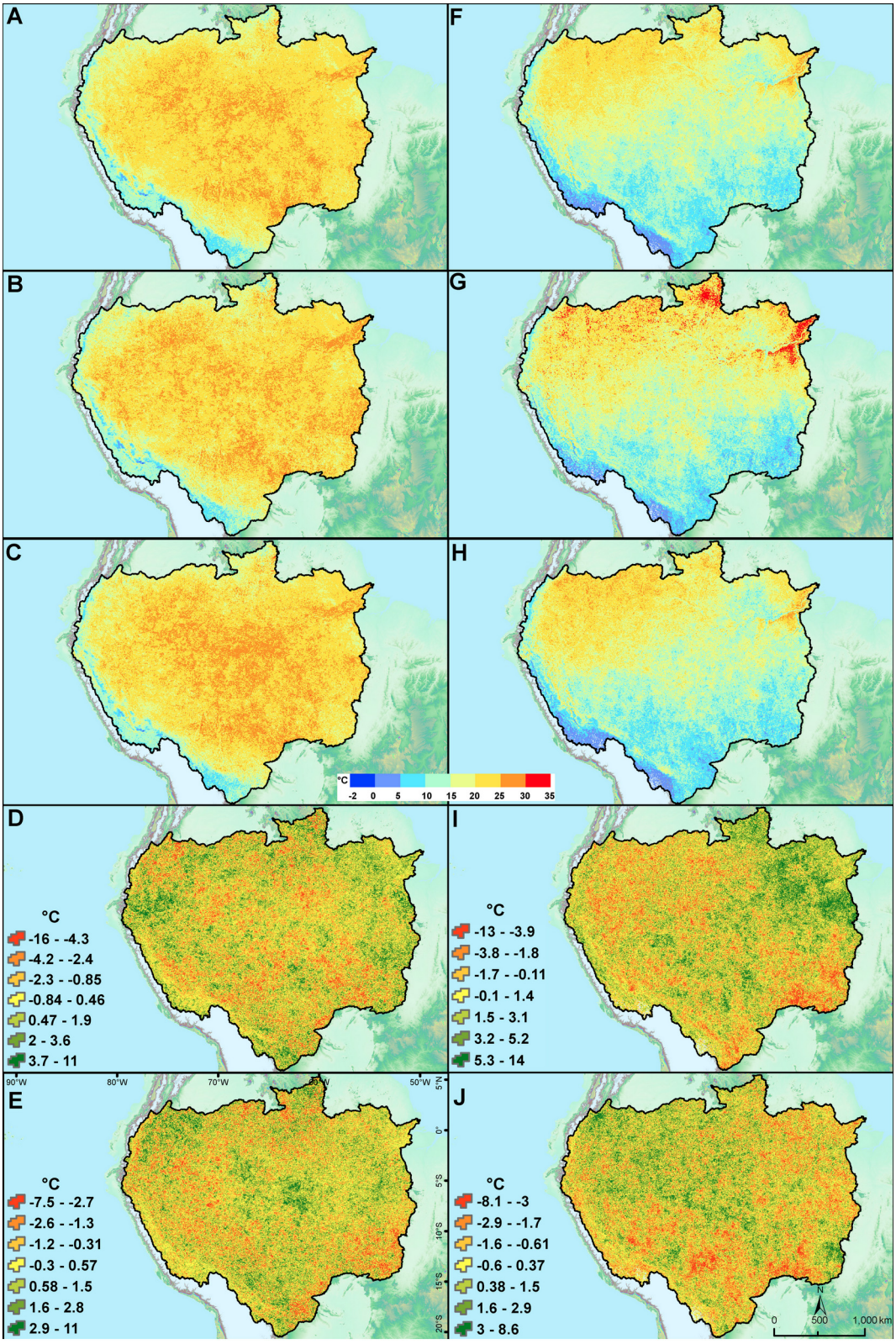

Fig. 5. Spatial variations of temperature without presence of the phenomena in the rainier (A) and less rainy (F) months, temperature with the presence of La Niña in rainier (B) and less rainy (G) months, temperature in the presence of El Niño in rainier (C) and less rainy (H) months, temperature increase and reduction with presence of La Niña in rainier (D) and less rainy (I) periods and presence of El Niño in rainier (E) and less (J) rainy periods.

4.3. Evapotranspiration

The monthly evapotranspiration variation showed that among the ten lowest values, eight of them were associated with LN and two with EN, so the low evapotranspiration rates refer to LN events. Of the ten highest values in the historical series, six occurred in EN, two in LN and two in Neutral periods, highlighting the influence of EN on the increase of values. It is significant that 2009 presented the highest evapotranspiration values of the period and was proceeded by an extreme drought event in the Amazon

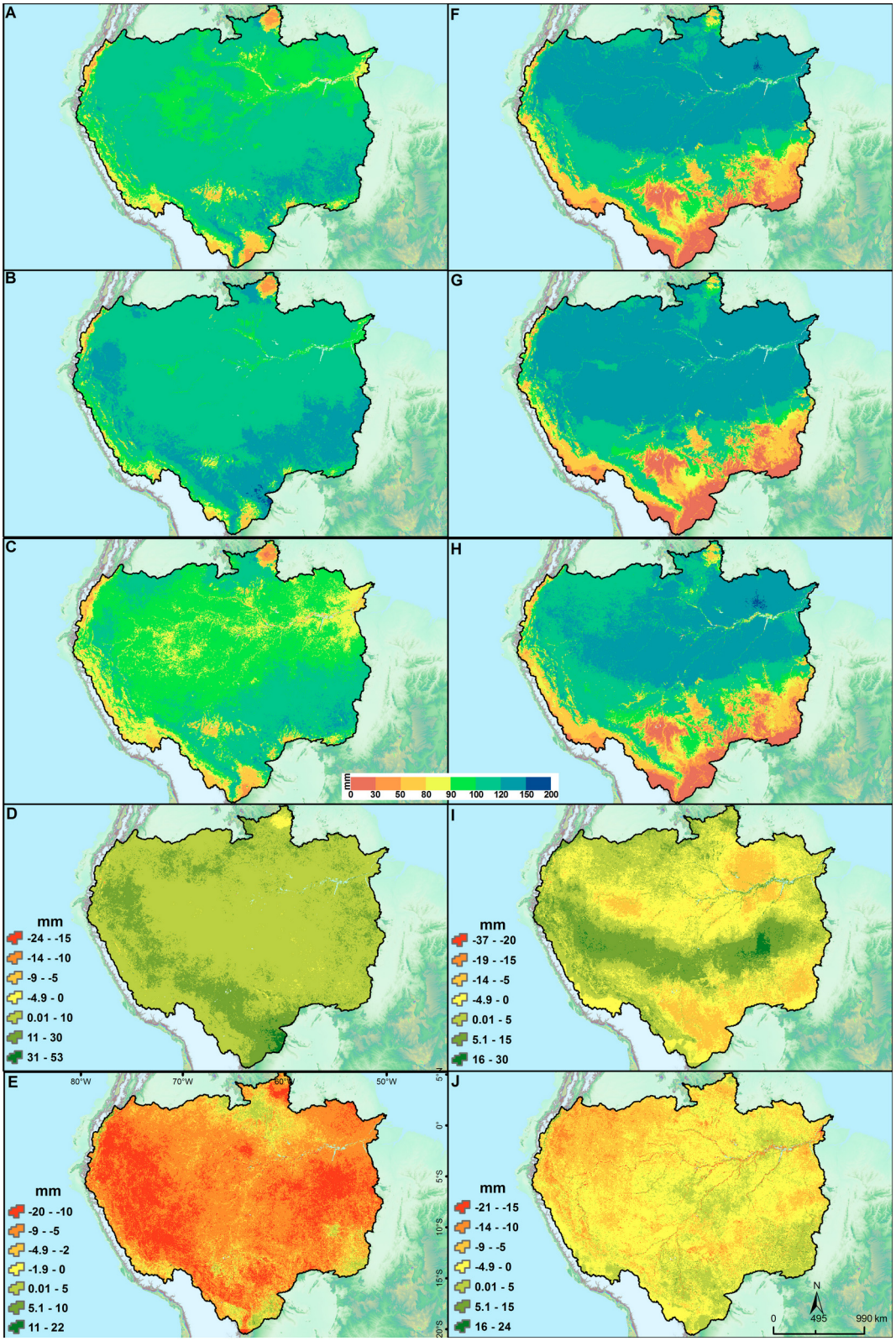

Fig. 6. Spatial variations of evapotranspiration without presence of the phenomena in the rainiest (A) and less rainy (F) months, evapotranspiration with La Niña presence in rainier (B) and less rainy (G) months, evapotranspiration with El Niño presence in rainier (C) and less rainy months (H), increase and reduction of the evapotranspiration with the presence of La Niña in rainier (D) and less rainy (I) periods and presence of El Niño in rainier (E) and less rainy (J) periods.

region, with Marengo et al. (2011) highlighting that the drought in 2010 occurred in substitution for the cold phase (La Niña). Given this, the EN may change the climatic variables, favoring the occurrence of severe droughts in the Amazon region. Similarly, evapotranspiration observation over an annual timeframe shows values above the historical averages since 2006, and its occurrence was independent of the presence of the phenomena. Carmona et al. (2016) and Khand et al. (2017) have concluded that changes of this magnitude are associated with changes in land use caused by anthropogenic pressures.

The temporal analysis of the annual averages showed a trend line with an increasing pattern, indicating an increase in evapotranspiration over the years with a difference of 6.53 mm between 2000 and 2016, and an increase of approximately 0.38 mm per year. According to Flantua et al. (2015) and IPCC (2014), this annual increase is related to the increase in the vapor pressure deficit that is a result of the temperature increase. The evapotranspiration variations in the neutral periods, in months of high and low precipitation. It is possible to observe the variation between the minimum and maximum evapotranspiration values. As a result, the lowest values are concentrated in the southeastern region of the study area where the highest areas are located; therefore, it is more affected by the solar incidence, which is an evapotranspiration limiting factor. In this region, values ranged from 0 to 80 mm, values which are below the average for this basin.

Analyzing the images of the periods with the occurrence of the LN phenomenon during months with higher and lower pluviometric precipitation intensities, it was found that the observed values were higher when compared to the Neutral and EN periods. In the periods with more pluviometric precipitation, the values varied in most of the basin between 100 and 120 mm, but in the months with less rainfall the variation increased from 120 to 150 mm, showing values above those observed for the Neutral and EN periods. Therefore, reductions in evapotranspiration are explained by changes in the rainy season due to the LN phenomenon, whereas in the less rainy months, the reduction of humidity together with the elevation of temperature causes an increase in evapotranspiration rates (Flantua et al., 2015; Nobre et al., 2013).

The differences between the Neutral and LN periods where the greatest reductions in evapotranspiration were concentrated in the northern region, with values decreasing by as much as 24 mm. In the rest of the basin there were increases ranging from 0.01 to 30 mm. In the less rainy months in much of the basin, there were reductions of 4.9 mm to 19 mm, except for the central region, which was affected by increases of between 5.1 mm and 30 mm. In this way, it can be said that the greatest evapotranspiration reductions occurred in the presence of the LN phenomenon, mainly in the months with lower rainfall intensities, provided by lower temperatures and drier air (Khand et al., 2017; Silva et al., 2015). The differences between the Neutral periods and the EN phenomena with higher and lower rainfall intensities, with reductions of as much as 20 mm and increases of up to 22 mm in the presence of the EN phenomenon being observable. In the periods with the lowest rainfall intensities, the variation was −21 mm to 24 mm.

In general, the months with the lowest rainfall were those with the highest mean evapotranspiration, concentrating in the central and northern regions of the study area. This region presents fewer anthropic pressures and has denser vegetation cover, therefore, it has higher incidence of solar radiation, increasing vegetative transpiration and evaporation from water bodies, consequently, conditioning an increment in the evapotranspiration. This is different to what occurs during rainier periods, where the presence of greater cloud cover inhibits the incidence of solar radiation, decreasing the temperature and consequently reducing evapotranspiration (Flantua et al., 2015).

5. Conclusions

Based on the results obtained it was concluded that:

Monthly precipitation averages are reduced as a result of the EN phenomenon, while in this same period there is an increase in temperature and evapotranspiration averages. In the presence of the LN phenomenon, opposite variations were observed.

El Niño occurred in the middle of 2015–2016 with strong intensity that was crucial to increase temperatures and reduce pluviometric precipitation.

The trend lines of the meteorological variables generated from the annual data showed reductions in precipitation and temperature and evapotranspiration increases between 2000 and 2016, corroborating data predicted by the IPCC.

In general, the presence of LN increased precipitation values in comparison to the Neutral period, and the inverse occurs in the presence of EN.

The periods with lower rainfall intensities were more affected by the phenomena, in comparison with those with higher intensities. Despite this, no variations were observed in minimum temperatures in years presenting EN influence.

In the months characterized by the presence of EN, the lowest temperatures of the studied period were observed in the south and southwest regions of the basin. In the central region, there was an increase in the values of this variable.

El Niño caused the greatest temperature differences in comparison with LN and Neutral periods, leading to values above or below average.

The analysis of the rainy periods showed a variation of the evapotranspiration in the presence of the phenomena, but LN generated above average values in the basin, the opposite to what was observed during EN.

The presence of EN in less rainy months caused reductions in temperature and evapotranspiration in almost the whole basin, an inverse result to that observed in the presence of LN.

This methodology was adequate to analyze the modifications of the meteorological variables coming from the EN and LN phenomena, being able to be adapted to other variables and areas.

Acknowledgments

The authors are grateful to the Integrated System for National Aeronautics and Space Administration (NASA), National Oceanic and Atmospheric Administration (NOAA), to the CNPq research group Geotechnology Applied to Global Environment (GAGEN), to the Coordination of Improvement of Higher Education Personnel (CAPES) and the Postgraduate Program in Forest Sciences of the Federal University of Espirito Santo for providing the necessary resources for implementation and execution of this work.

References

Almeida, C.T., Oliveira-Júnior, J.F., Delgado, R.C., Cubo, P., Ramos, M.C., 2017. Spatiotemporal rainfall and temperature trends throughout the Brazilian Legal Amazon, 1973–2013. Int. J. Climatol. 37, 2013–2026. https://doi.org/10.1002/joc.4831.

Alves, D.B., Pérez-Cabello, F., 2017. Multiple remote sensing data sources to assess spatiotemporal patterns of fire incidence over Campos Amazônicos Savanna Vegetation Enclave (Brazilian Amazon). Sci. Total Environ. 601–602, 142–158. https://doi.org/10.1016/j.scitotenv.2017.05.194.

Ayala, L.M., van Eupen, M., Zhang, G., Pérez-Soba, M., Martorano, L.G., Lisboa, L.S., Beltrao, N.E., 2016. Impact of agricultural expansion on water footprint in the Amazon under climate change scenarios. Sci. Total Environ. 569–570, 1159–1173. https://doi.org/10.1016/j.scitotenv.2016.06.191.

Cai, W., Borlace, S., Lengaigne, M., Van Rensch, P., Collins, M., Vecchi, G., Timmermann, A., Santoso, A., Mcphaden, M.J., Wu, L., England, M.H., Wang, G., Guilyardi, E., Jin, F.F., 2014. Increasing frequency of extreme El Niño events due to greenhouse warming. Nat. Clim. Chang. 4, 111–116. https://doi.org/10.1038/nclimate2100.

Carmona, A.M., Poveda, G., Sivapalan, M., Vallejo-Bernal, S.M., Bustamante, E., 2016. A scaling approach to Budyko's framework and the complementary relationship of evapotranspiration in humid environments: case study of the Amazon River basin. Hydrol. Earth Syst. Sci. 20, 589–603. https://doi.org/10.5194/hess-20-589-2016.

de Sousa, A.M.L., da Rocha, E.J.P., Vitorino, M.I., de Souza, P.J.O.P., Botelho, M.N., 2015. Variabilidade espaço-temporal da precipitação na amazônia durante eventos enos. Rev. Bras. Geogr. Física 8, 13–24.

dos Santos, S.R.Q., Sansigolo, C.A., Neves, T.T. de A.T., Campos, T.L. de O.B., dos Santos, A.P.P., 2017. Frequências dos eventos extremos de seca e chuva na Amazônia utilizando diferentes bancos de dados de precipitação. Rev. Bras. Geogr. Física 10, 468–478. https://doi.org/10.5935/1984-2295.20140015.

Fan, J., Meng, J., Ashkenazy, Y., Havlin, S., Schellnhuber, H.J., 2017. Network analysis reveals strongly localized impacts of El Niño. Proc. Natl. Acad. Sci. 114, 7543–7548. https://doi.org/10.1073/pnas.1701214114.

Fernando, F., Marcuzzo, N., Romero, V., 2013. INFLUÊNCIA DO EL NIÑO E LA NIÑA NA PRECIPITAÇÃO MÁXIMA DIÁRIA DO ESTADO DE GOIÁS CPRM/SGB - Serviço Geológico do Brasil, Porto Alegre, RS, Brasil Instituto Federal de Educação, Ciência e Tecnologia de Goiás (IFG), Goiânia, GO, Brasil. 1997 pp. 429–440.

Flantua, S.G.A., Hooghiemstra, H., Vuille, M., Behling, H., Carson, J.F., Gosling, W.D., Hoyos, I., Ledru, M.P., Montoya, E., Mayle, F., Maldonado, A., Rull, V., Tonello, M.S., Whitney,

B.S., González-Arango, C., 2015. Climate variability and human impact on the environment in South America during the last 2000 years: synthesis and perspectives. Clim. Past Discuss. 11, 3475–3565. https://doi.org/10.5194/cpd-11-3475-2015.
Foley, J.A., Botta, A., Coe, M.T., Costa, M.H., 2002. El Niño-Southern oscillation and the climate, ecosystems and rivers of Amazonia. Glob. Biogeochem. Cycles 16. https://doi.org/10.1029/2002GB001872 (79-1-79–20).
Fujii, Y., Kamachi, M., Nakaegawa, T., Yasuda, T., Yamanaka, G., Toyoda, T., Ando, K., 2012. Assimilating Ocean Observation Data for ENSO Monitoring and Forecasting. Tech Open.
ggweather, 2008. Golden gate weather services [WWW document]. ENSO Years Based Ocean. Niño Index http://ggweather.com/enso/oni.htm.
Hua, L., Lu, Z., Yuan, N., Chen, L., Yu, Y., Wang, L., 2017. Percolation phase transition of surface air temperature networks: a new test bed for El Niño/La Niña simulations. Sci. Rep. 7 (8324). https://doi.org/10.1038/s41598-017-08767-4.
Huang, X., Deng, J., Wang, W., Feng, Q., Liang, T., 2017. Impact of climate and elevation on snow cover using integrated remote sensing snow products in Tibetan Plateau. Remote Sens. Environ. 190, 274–288. https://doi.org/10.1016/j.rse.2016.12.028.
INPE, 2017. Instituto Nacional de Pesquisas Espaciais [WWW Document]. Portal do Monit. Queimadas e Incêndios. http://www.inpe.br/queimadas.
IPCC, 2014. Climate change 2014 synthesis report. Contrib. Work. Groups I, II III to Fifth Assess. Rep. Intergov. Panel Clim. Chang, pp. 1–151.
Ji, D., Shi, J., Xiong, C., Wang, T., Zhang, Y., 2017. A total precipitable water retrieval method over land using the combination of passive microwave and optical remote sensing. Remote Sens. Environ. 191, 313–327. https://doi.org/10.1016/j.rse.2017.01.028.
Khand, K., Numata, I., Kjaersgaard, J., Vourlitis, G.L., 2017. Dry season evapotranspiration dynamics over human-impacted landscapes in the southern Amazon using the landsat-based METRIC model. Remote Sens. 9. https://doi.org/10.3390/rs9070706.
Li, W., Zhang, P., Ye, J., Baker, P.A., 2010. Impact of two different types of el nino events on teh amazon climate ad ecosystem productivity. Oxford J. 4, 91–99. https://doi.org/10.1093/rtq039.
Liberato, A.M., de Brito, J.I.B., 2011. Influência de mudanças climáticas no balanço hídrico da amazônia ocidental. Rev. Bras. Geogr. Física 06, 1275–1291.
Lin, H., Chen, Y., Song, Q., Fu, P., Cleverly, J., Magliulo, V., Law, B.E., Gough, C.M., Hörtnagl, L., Di Gennaro, F., Matteucci, G., Montagnani, L., Duce, P., Shao, C., Kato, T., Bonal, D., Paul-Limoges, E., Beringer, J., Grace, J., Fan, Z., 2017. Quantifying deforestation and forest degradation with thermal response. Sci. Total Environ. 607–608, 1286–1292. https://doi.org/10.1016/j.scitotenv.2017.07.062.
Marengo, J.A., Nobre, C.A., Tomasella, J., Oyama, M.D., de Oliveira, G.S., de Oliveira, R., Camargo, H., Alves, L.M., Brown, I.F., 2008. The drought of Amazonia in 2005. J. Clim. 21, 495–516. https://doi.org/10.1175/2007JCLI1600.1.
Marengo, J.A., Tomasella, J., Alves, L.M., Soares, W.R., Rodriguez, D.A., 2011. The drought of 2010 in the context of historical droughts in the Amazon region. Geophys. Res. Lett. 38, 1–5. https://doi.org/10.1029/2011GL047436.
Mokhov, I.I., Smirnov, D.A., 2016. Relation between the variations in the global surface temperature, El Niño/La Niña phenomena, and the Atlantic Multidecadal Oscillation. Dokl. Earth Sci. 467, 384–388. https://doi.org/10.1134/S1028334X16040115.
Moreira, M.A., 2011. Fundamentos do sensoriamento remoto e metodologias de aplicação. 4a. ed. UFV, Viçosa, MG.
NOAA, 2017. National Weather Service: Cold & Warm Episodes by Season, Climate Prediction Center [WWW Document].
Nobre, C.A., Obrégon, G.O., Marengo, J.A., 2013. The Amazonian boundary layer and mesoscale circulations. Amaz. Glob. Chang. 163–181. https://doi.org/10.1029/2008GM000720.
Oliveira, N.D.L., Marcuzzo, F.F.N., Barros, R.G., 2015. Influência do El Niño e La Niña no número de dias de precipitação pluviométrica no Estado do Mato Grosso Influence of El Niño and La Niña in the number of days of rainfall in the state of Mato Grosso. Introdução O Mato Grosso concentra boa parte da econo. 1982 pp. 284–297.
Panisset, J.S., Gouveia, C.M., Libonati, R., Peres, L., Machado-silva, F., 2017. Evaluation of last extreme drought events in Amazon basin using remotely sensing data. Egu 19, 16144.
Ponzoni, F.J., Shimabukuro, Y.E., Kuplich, T.M., 2012. Sensoriamento remoto da vegetação, 2a edição. ed. Oficina de Textos, São Paulo.
Running, S.W., Mu, Q., Zhao, M., Moreno, Alvaro, 2017. User's Guide MODIS Global Terrestrial Evapotranspiration (ET) Product (NASA MOD16A2/A3) 35.
Serrão, E.A. de O., dos Santos, C.A., Wanzeler, R.T.S., Gonçalves, L. de J.M., de Lima, A.M.M., 2015. Avaliação da seca de 2005 e 2010 na Amazônia: análise da bacia hidrográfica do rio Solimões. Rev. Geogr. Acadêmica 9, 5–20.
Silva, H.J.F., Lucio, P.S., Brown, I.F., 2015. Análise mensal, sazonal e interanual da evapotranspiração de referência para o sudoeste da Amazônia, Acre, Brasil. Rev. Bras. Geogr. Física 08, 1711–1729. https://doi.org/10.5935/1984-2295.20140015.
Trenberth, K.E., 1984. Signal versus noise in the southern oscillation. Mon. Weather Rev. https://doi.org/10.1175/1520-0493(1984)112<0326:SVNITS>2.0.CO;2.
Trenberth, K.E., 1997. The definition of El Niño. Bull. Am. Meteorol. Soc. 78, 2771–2777. https://doi.org/10.1175/1520-0477(1997)078<2771:TDOENO>2.0.CO;2.
Trenberth, K.E., Stepaniak, D.P., 2001. Indices of El Nino evolution. J. Clim. 14, 1697–1701. https://doi.org/10.1175/1520-0442(2001)014<1697:LIOENO>2.0.CO;2.
Viers, J., Barroux, G., Pinelli, M., Seyler, P., Oliva, P., Dupré, B., Boaventura, G.R., 2005. The influence of the Amazonian floodplain ecosystems on the trace element dynamics of the Amazon River mainstem (Brazil). Sci. Total Environ. 339, 219–232. https://doi.org/10.1016/j.scitotenv.2004.07.034.
Wan, Z., 2013. MODIS land surface temperature products users' guide. NASA EOSDIS L. Process. 33. DAAC. https://doi.org/10.5067/MODIS/MOD11B3.006.